International Journal of Solids and Structures 47 (2010) 2034–2042

Contents lists available at ScienceDirect

International Journal of Solids and Structures

journal homepage: www.elsevier.com/locate/ijsolstr

Humidity-driven bifurcation in a hydrogel-actuated nanostructure: A three-dimensional computational analysis

W.H. Wong [a], T.F. Guo [b,*], Y.W. Zhang [b,c], L. Cheng [a,**]

[a] Department of Mechanical Engineering, National University of Singapore, Singapore 117576, Singapore
[b] Institute of High Performance Computing, Singapore 138632, Singapore
[c] Department of Materials Science and Engineering, National University of Singapore, Singapore 117574, Singapore

ARTICLE INFO

Article history:
Received 2 February 2010
Received in revised form 25 March 2010
Available online 9 April 2010

Keywords:
Hydrogel
Humidity-driven bifurcation
Nanostructure
Inhomogeneous deformation

ABSTRACT

Hydrogel-based adaptive structures that respond to specific external stimuli present immense potential for applications in microfluidics, shape-memory devices, artificial muscle and actuators. Using a three-dimensional finite element method, we analyse the humidity-driven bifurcation of a nanostructure, made up of periodically distributed nanoscale rods embedded vertically in a swollen hydrogel layer. The bifurcation manifests as a switching behavior of the nanorods between vertical and tilted states. The use of representative volume element with realistic boundary conditions allows us to fully consider inhomogeneous deformations of the hydrogel. Our computations reveal that at higher initial swelling ratio, the bifurcation behavior of the nanostructure approaches that of the case where homogeneous deformation in the hydrogel is considered. However, large deviation in the behavior may occur between the two at lower initial swelling ratio. We further investigate quantitatively the effects of geometrical and material variations on the bifurcation behavior. It is found that geometric-material parameters can significantly affect the critical switching state and its post-bifurcation behavior, enabling great tunability in the design and application of hydrogel-based adaptive nanostructure.

1. Introduction

Stimuli-responsive materials and structures have received considerable attention in many fields of research, from medicine and biology to chemistry, physics, materials science and engineering. Stimulus or external applied field may include humidity, pH, thermal, magnetic, electrical, ultraviolet/visible light or combinations thereof (Ahn et al., 2008; Russell, 2002). Hydrogels are prominent examples of such adaptive materials capable of large and reversible deformations. Hydrogels are composed of cross-linked flexible polymeric hydrophilic chains whose elastic networks are able to swell when hydrated. These structures are typically miniaturized so as to achieve fast response to minute changes in solvent concentration. These artificial responsive materials have been shown to exhibit potential applications in microfluidics (Beebe et al., 2000), as shape-memory materials (Osada and Matsuda, 1995), artificial muscles and actuators (Hirai, 2007; Osada et al., 1992) and optical switches (Pardo-Yissar et al., 2001).

Indeed, the designs of such structures are inspired by nature's very own biological and functional structures. For example, nano- and microstructures that developed on surfaces of lotus leaves and gecko feet provide these organisms with exceptional water-repelling and adhesion properties respectively (Barthlott and Neinhuis, 1997; Autumn et al., 2002). Common to these seemingly unrelated features is the presence and use of fibres and high-aspect-ratio nano- and microstructures. Nanostructures that mimic these biological structures and functions have been artificially produced (Geim et al., 2003; Sidorenko et al., 2008; Pokroy et al., 2009), where nanocolumns of high aspect ratio are integrated with hydrogels. The formation of complex micropatterns through the reversible switching and actuation of the nanostructures has also been demonstrated (Sidorenko et al., 2007). These hydrogels provide the "muscle" to reversibly actuate the nanostructures, changing their orientation in response to changes in humidity levels. The actuation of the nanostructures is brought about the nonlinear, inhomogeneous deformation of the hydrogel as a result of the mechanical constraint imposed on the structure (De et al., 2002; Zhao et al., 2008).

By analogy to the phase transition in statistical mechanics, Hong et al. (2008a) examined the free-energy of hydrogels for bifurcation of a homogeneous deformation field from vertical standing state to tilted state. They succeeded in finding a nontrivial solution that can qualitatively describe the switching behavior/bifurcation of a hydrogel-actuated nanostructure. In the analysis, the deformation in the hydrogel is assumed to be homogeneous,

* Corresponding author.
** Corresponding author. Tel.: +65 65166888; fax: +65 67791459.
E-mail addresses: guotf@ihpc.a-star.edu.sg (T.F. Guo), mpecl@nus.edu.sg (L. Cheng).

0020-7683/$ - see front matter © 2010 Elsevier Ltd. All rights reserved.
doi:10.1016/j.ijsolstr.2010.03.036

with the deformation gradient tensor F_{iK} taken to be a constant tensor. In reality, inhomogeneous deformations are induced in the hydrogel due to the nanorods and should be taken into account in order to gain a deeper insight to the bifurcation behavior of the actuator.

Continuum models of hydrogels have been developed for analyses of their responses to external stimuli or loads. Dolbow et al. (2004) investigated phase interface transitions of chemically-induced swelling and de-swelling of hydrogels, and provided numerical results that are qualitatively comparable to experimental observations. Their numerics are accomplished with a hybrid extended-finite-element/level-set method. Under the same token, Ji et al. (2006) analysed the kinetics of thermally-induced hydrogel swelling and predicted, in agreement with experimental results, the threshold temperatures for phase transitions of the hydrogel. An insight to the kinetics of temperature-sensitive hydrogels, including the flow fields of the solvent, is provided by Birgersson et al. (2008) using a generic biphasic model. A comprehensive and systematic description of modelling and simulation of the smart polymer hydrogels responding to various stimuli can be found in a recently published book authored by Li (2009).

The goal of this work is to examine the influences of nanostructural effects – geometric-material variations in the nanostructure – on the bifurcation and consequently its adaptive response, taking into account inhomogeneous deformation field in the structure. Section 2 outlines the material models used for the nanostructure. Section 3 details the modelling aspects of a representative volume element of the nanostructure. This is preceded by a review on the bifurcation of the nanostructure due to the homogeneous deformation of the hydrogel. In Section 4, we investigate the effects of several key geometric-material parameters on the bifurcation behavior of the nanostructure. A short summary in Section 5 concludes this paper.

2. Material model

The nanostructure consists of square arrays of vertically oriented, free-standing, high-aspect-ratio silicon nanorods integrated with a hydrogel layer, as illustrated in Fig. 1. This nanostructure is bonded to a stiff substrate. The nanorods are taken to be elastic with Young's modulus E_{rod} and Poisson's ratio υ_{rod}. The material behavior of the hydrogel is analogous to a compressible hyperelastic solid and can be described by free-energy functions. This section describes the free-energy function for the hydrogel.

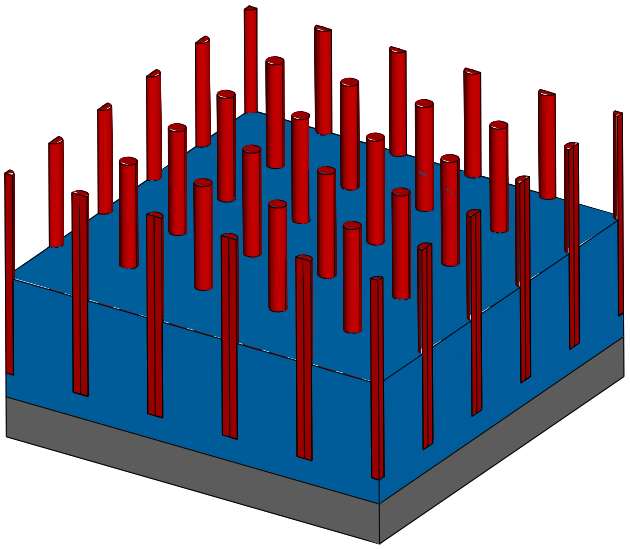

Fig. 1. A three-dimensional illustration of a section of the nanorod-embedded hydrogel structure.

Recently, the use of nonlinear field theories to analyse large deformations in hydrogels has been successfully demonstrated (Li et al., 2007; Hong et al., 2008b; Zhang et al., 2009). Coupled with free-energy functions for swelling elastomers, full-field analyses of boundary value problems involving hydrogels under various stimuli have been made possible, as what this paper seeks to achieve. Here, the well-known free-energy function due to Flory and Rehner (Flory and Rehner, 1943) is adopted, namely

$$W(F_{iK},C)=\frac{1}{2}NkT[F_{iK}F_{iK}-3-2\ln(\det(F_{iK}))]-\frac{kT}{\upsilon}\left[\upsilon C\ln\left(1+\frac{1}{\upsilon C}\right)+\frac{\chi}{1+\upsilon C}\right] \tag{1}$$

where N is the number of polymeric chains per reference volume, kT is the temperature in the unit of energy, υ is the volume per water molecule, C is the concentration of water molecules in the hydrogel and χ is a dimensionless measure of the enthalpy of mixing, an indicator of the ease of polymer–solvent interaction. F_{iK} is the deformation gradient of the hydrogel defined as

$$F_{iK}=\frac{\partial x_i(X_1,X_2,X_3)}{\partial X_K} \tag{2}$$

where X_K denote the coordinates of a material point in the reference configuration, while the functions $x_i(X_1,X_2,X_3)$ specify the coordinates of that point in the deformed configuration. In terms of principal stretches λ_1, λ_2 and λ_3, $F_{iK}F_{iK}=\lambda_1^2+\lambda_2^2+\lambda_3^2$ and $\det(F_{iK})=\lambda_1\lambda_2\lambda_3$. The deformation gradient tensor F_{iK} will be used to characterize the state of deformation of a point in the hydrogel.

The first term on the right-hand side of (1) is the elastic free-energy of the network in terms of principal stretches, while the second term is free-energy due to mixing of polymer and water molecules. Note that the first term is the familiar strain energy function for a neo-Hookean solid of shear modulus NkT. We designate the shear modulus by G_{gel}. The product υC is the volume of water imbibed in the network, and it arises from the assumption of incompressibility of individual polymeric and water molecules, such that the volume of the hydrogel equals the sum of individual molecules of the dry network and water. This gives the relation

$$1+\upsilon C=\det(F_{iK}) \tag{3}$$

The external stimulus of humidity is the chemical potential of water molecules in the environment

$$\mu=\frac{\partial W(F_{iK},C)}{\partial C} \tag{4}$$

which is work-conjugate to the concentration of water molecules C in the hydrogel (Hong et al., 2009). We will take the deformation gradient F_{iK} and the chemical potential of water molecules in the environment μ as independent variables in the free-energy function. To this end, we apply a Legendre transformation to $W(F_{iK},C)$, using (4), to give

$$W^*(F_{iK},\mu)=W(F_{iK},C)-\mu C \tag{5}$$

Inserting (1) and (3) into (5) and normalizing with kT/υ yields the free-energy function

$$\frac{\upsilon W^*(F_{iK},\mu)}{kT}=\frac{1}{2}N\upsilon[I-3-2\ln J]-(J-1)\ln\left(\frac{J}{J-1}\right)-\frac{\chi}{J}-\frac{\mu}{kT}(J-1) \tag{6}$$

where $I=F_{iK}F_{iK}$ and $J=\det(F_{iK})$. The chemical potential of water molecules in the saturated environment is taken to be zero. The chemical potential of water molecules in an unsaturated environment

relates to the relative humidity RH as $\mu = kT\ln(RH)$. Readers are referred to Hong et al. (2008a, 2009) for details on the theoretical framework of the field theory, the constitutive formulation and the numerical implementation.

3. Bifurcation of hydrogel-actuated nanostructure

This section formulates the boundary value problem for the bifurcation of the hydrogel-actuated nanostructure. We begin by reviewing the bifurcation behavior of a hydrogel as analysed by Hong et al. (2008a). Inferring from their works, we describe the numerical aspects of our analysis.

3.1. Homogeneous deformation of hydrogel

Following the experimental works of Sidorenko et al. (2007), Hong et al. (2008a) analysed the bifurcation of the hydrogel-actuated nanostructure by considering homogeneous deformation of the hydrogel. We recapitulate some aspects of their work, as their results will be used for a comparative study later in the paper.

Nanoscale rods are embedded in a hydrogel, which is attached to a stiff substrate. The hydrogel is initially water-free and stress-free and this state is taken to be the reference state. The nanorods stand vertical when the hydrogel has imbibed water and swelled with an isotropic swelling ratio λ_0. During the drying process, the hydrogel shrinks and causes the nanorods to tilt by θ, as shown schematically in Fig. 2. Referring to the Cartesian frame shown, the coordinates of a material point in the hydrogel in the swollen state, with respect to the reference state, is given by $(\lambda_0 X_1, \lambda_0 X_2, \lambda_0 X_3)$. In the tilted state, this material point occupies a new position whose coordinates are $(\lambda_0(X_1 + X_3\ \sin\theta), \lambda_0 X_2, \lambda_0 X_3 \cos\theta)$. In view of (2), the resulting deformation gradient tensor can be expressed in the matrix form as

$$(F_{iK}) = \lambda_0 \begin{pmatrix} 1 & 0 & \sin\theta \\ 0 & 1 & 0 \\ 0 & 0 & \cos\theta \end{pmatrix} \tag{7}$$

The volume of the hydrogel in the tilted state with respect to the reference state is

$$\det(F_{iK}) = \lambda_0^3 \cos\theta \tag{8}$$

indicating that the tilt causes the hydrogel to shrink in volume relative to the vertical state and allows the hydrogel to release water.

At this juncture, it is worthwhile to remark that the matrix in (7) can be decomposed into two parts

$$\begin{pmatrix} 1 & 0 & \sin\theta \\ 0 & 1 & 0 \\ 0 & 0 & \cos\theta \end{pmatrix} = \begin{pmatrix} 1 & 0 & \tan\theta \\ 0 & 1 & 0 \\ 0 & 0 & 1 \end{pmatrix} \begin{pmatrix} 1 & 0 & 0 \\ 0 & 1 & 0 \\ 0 & 0 & \cos\theta \end{pmatrix} \tag{9}$$

The first matrix on the right-hand side of (9) signifies a simple shear, while the second a volume reduction in the X_3-direction, that is, a vertical shrink. A physical interpretation that can be assigned to the multiplicative decomposition of F_{iK} is that as the environment dries, the hydrogel first undergoes a vertical shrinking, followed by a simple shear.

Inserting (7) and (8) into (6) gives

$$\frac{\upsilon W^*(\theta,\mu)}{kT} = \frac{1}{2}N\upsilon\left[3(\lambda_0^2 - 1) - 2\ln(\lambda_0^3\cos\theta)\right] + (\lambda_0^3\cos\theta - 1)\left(\ln\frac{\lambda_0^3\cos\theta - 1}{\lambda_0^3\cos\theta} - \frac{\mu}{kT}\right) - \frac{\chi}{\lambda_0^3\cos\theta} \tag{10}$$

The total energy is minimised as the structure equilibrates. Differentiating (10) with respect to θ and equating the derivative to zero yields

$$\frac{\mu}{kT} = \frac{1 - N\upsilon}{\lambda_0^3\cos\theta} + \ln\frac{\lambda_0^3\cos\theta - 1}{\lambda_0^3\cos\theta} + \frac{\chi}{(\lambda_0^3\cos\theta)^2} \tag{11}$$

The equation, hereafter referred to as HZS, relates the tilt angle to the chemical potential of the system (and hence RH). There exists a humidity level, defined as the critical humidity RH_c, at which the nanorods stand vertical ($\theta = 0$). RH_c is obtained by setting $\theta = 0$ in HZS,

$$\frac{\mu_c}{kT} = \frac{1 - N\upsilon}{\lambda_0^3} + \ln\frac{\lambda_0^3 - 1}{\lambda_0^3} + \frac{\chi}{\lambda_0^6} \tag{12}$$

where μ_c is the *critical* chemical potential and consequently, the critical humidity. For any given set of parameters of $N\upsilon$, λ_0 and χ, HZS indicates that the nanorods will stand vertical for humidity levels above RH_c. However, the nanorods will tilt by a large angle when the humidity of the environment drops slightly below RH_c. RH_c therefore sets the condition for the onset of bifurcation and HZS describes the post-bifurcation behavior.

3.2. Inhomogeneous deformation of hydrogel and modelling aspects

Bifurcation behavior predicted by HZS assumes the hydrogel is under a constant state of homogeneous deformation during the drying process, and the controlling material parameters in HZS pertain to the hydrogel. In reality, the hydrogel undergoes inhomogeneous deformation on its top surface and near the bottom of the

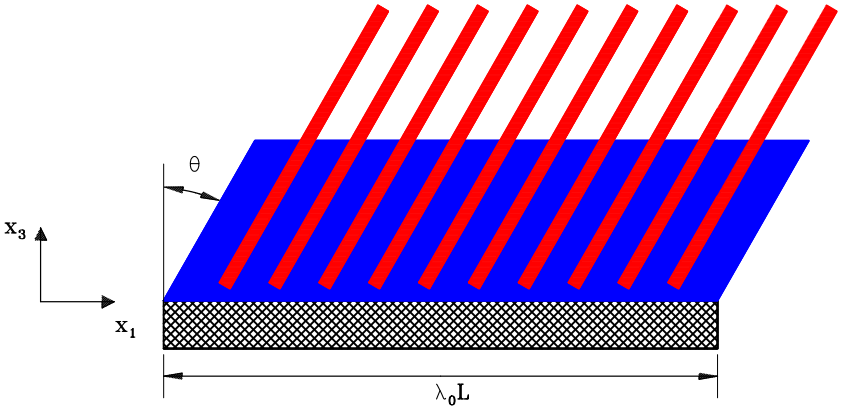

Fig. 2. Schematic illustrating the tilted state of nanorods. The initially swollen hydrogel undergoes a volume reduction in X_3-direction followed by a simple shear. Deformation due to simple shear results in the tilting of the nanorods.

nanorods. Inhomogeneous deformation of hydrogel has been observed experimentally (Sidorenko et al., 2007). Nanostructural effects such as those of moduli mismatch between the nanorods and the surrounding hydrogel and spatial distribution of the nanorods, parameters that are often design concerns of hydrogel-based actuators, contribute to the inhomogeneous deformation in the hydrogel. Based on the theoretical analysis by Hong et al. (2008a), we seek to provide an analysis of the bifurcation behavior of the hydrogel undergoing inhomogeneous deformation in a continuum scale. This section describes the modelling and numerical aspects.

To realistically model the nanostructural effects, we perform a three-dimensional analysis on a representative volume element of the nanostructure. By taking advantage of symmetry, we choose a representative volume element (RVE) of cross-sectional dimensions a by a, as shown in Fig. 3a. a is defined as the spacing between two adjacent nanorods measured from their centerlines. Fig. 3b displays, not drawn to scale, the RVE in the $X_1 - X_3$ plane. Each nanorod is of height h and diameter d. The thickness of the hydrogel layer is denoted by t_2. The nanorods protrude from the hydrogel and it is assumed that their exposed heights are uniform. The exposed height is denoted by t_1.

In this numerical study, we take the swollen state of the hydrogel as the reference state. Consequently, λ_0 is a prescribed parameter, representing the initial swelling ratio. In light of (7) and with reference to the Cartesian frames in Fig. 3a and b, we impose displacements

$$u_1 = (\sin\theta)X_3, \quad u_2 = 0, \quad u_3 = (\cos\theta - 1)X_3 \tag{13}$$

along $X_2 - X_3$ planes for $X_1 = 0$ and $X_1 = a$. Displacements $u_1 = u_2 = u_3 = 0$ are imposed along $X_1 - X_2$ plane for $X_3 = 0$, due to the confining surface of the substrate. Plane strain conditions are assumed and as such, displacement $u_2 = 0$ are imposed along $X_1 - X_3$ planes for $X_2 = 0$ and $X_2 = a$. In addition, traction-free conditions are assumed on plane $X_1 - X_2$ for $X_3 \geqslant t_2$. These conditions result in the inhomogeneous deformation of the hydrogel.

Our work explores the bifurcation behavior of the hydrogel-based nanostructure in response to a drying environment, taking into account of the inhomogeneous deformation in the structure. Specifically, we seek the relationship between the tilt angle of the nanorods θ and the corresponding relative humidity RH at equilibrium. In addition, we determine the critical humidity RH_c at which the nanorods stand vertical, as RH_c determines the onset of bifurcation and imposes a range of humidity levels at which nanorod switching is possible.

The numerical procedure involves seeking nonzero solutions of θ and RH for which the free-energy function (6) is convergent, and the corresponding total strain energy (SE) of the system attains a global minimum. Denoting θ_{trial} as the trial tilt angle in the iterations, for any prescribed RH, θ_{trial} is incrementally varied and the corresponding total SE evaluated. This iterative procedure, analogous to the root-finding algorithm of the bisection method, terminates when the total SE achieves a minima, yielding a solution pair of (RH, θ). Initial increments of θ_{trial} are set at 0.1 radians and are subsequently reduced to 0.01 rad as the minimum SE is approached. The range of RH considered is such that a minimum of 20 solution pairs of (RH, θ) are obtained.

The numerical iterations are performed within the finite strain settings using ABAQUS 6.8, with the material behavior of the hydrogel defined by the user-defined subroutine UHYPER. Fig. 3c displays the three-dimensional finite element mesh of the adopted RVE. The hydrogel is meshed with 8-node linear brick elements while the nanorods with 6-node linear wedge elements. The interfaces between the nanorods and the hydrogel are assumed to be fully bonded.

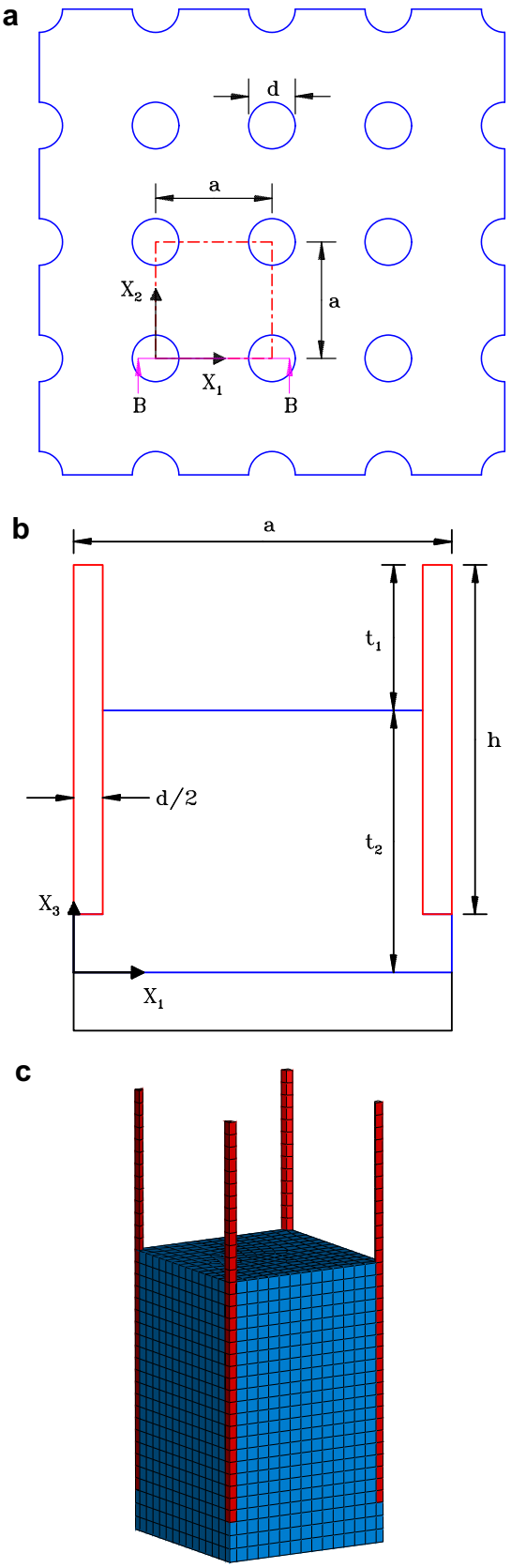

Fig. 3. (a) Cross-sectional view of the representative volume element (RVE) in the X_1–X_2 plane, as demarcated by dashed line, (b) cross-sectional view B–B in X_1–X_3 plane illustrating the notated dimensions, and (c) a finite element mesh of the RVE. A combination of 8-node linear brick and 6-node linear wedge elements are used.

4. Results and discussion

The influence of several geometric-material variations on the bifurcation behavior of the nanostructure under a state of inhomogeneous deformation is examined in this section. From dimensional considerations, the tilt angle θ of the nanorod depends on the following dimensionless geometric-material parameters:

$$\theta = F\left(\frac{\mu}{kT};\ \frac{G_{\text{rod}}}{G_{\text{gel}}}, \frac{a}{d}, \frac{h}{d}, \frac{t_1}{d}, \frac{t_2}{d};\ \lambda_0, \chi\right) \tag{14}$$

Our parametric study focuses on the shear modulus mismatch between nanorod and hydrogel $G_{\text{rod}}/G_{\text{gel}}$, the spacing between adjacent nanorods a/d, the initial swelling ratio of hydrogel λ_0 and the polymer–solvent parameter χ.

The hydrogel takes on the following material properties; the parameter χ has representative values of 0–1.2, while its shear modulus $G_{\text{gel}} = NkT$ takes on typical values of $10^4 - 10^7$ Pa. With the representative volume per molecule taken as $\upsilon = 10^{-28}$ m^3, and $kT = 4 \times 10^{-21}$ J at room temperature, $N\upsilon$ will have a range from $10^{-4} - 10^{-1}$. Guided by Sidorenko et al. (2007), the nanorods have diameters $d = 100 - 300$ nm, heights $h = 5 - 8$ μm, and spacing $a = 2 - 4$ μm. Throughout this paper, we take $N\upsilon = 0.1$, $\chi = 0.1$, $h/d = 25$, $a/d = 10$, $t_1/d = 10$ and $t_2/d = 17.5$, unless otherwise stated. The properties of nanorods are specified by Young's modulus $E_{\text{rod}} = 5.2$ GPa and Poisson's ratio $\nu_{\text{rod}} = 0.3$.

4.1. Effects of inhomogeneous deformation on bifurcation

We introduce the subject under discussion by displaying a plot of tilt angle θ as a function of relative humidity RH for initial swelling ratio of $\lambda_0 = 1.2$ and 1.6, as shown in Fig. 4. From this bifurcation diagram, it is observed that the bifurcation behavior of the nanostructure undergoing inhomogeneous deformation deviates from that of homogeneous deformation, as predicted by HZS and represented by dotted lines. On closer examination, the observed deviation more significant at lower level of λ_0. For $\lambda_0 = 1.2$, the values of RH_c determined numerically and from HZS are approximately 67% and 73%, respectively, giving a difference of about 8%. In the post-bifurcation regime, this difference can be greater than 10%. At higher level of $\lambda_0 = 1.6$, the effects of inhomogeneous deformation in the nanostructure become less apparent as RH_c and the post-bifurcation behavior converges towards HZS. For example, RH_c obtained numerically and from HZS are about 93% and 95%, respectively. This may be due to higher internal stresses generated as a result of larger volume of water imbibed, which acts to counteract the effects of the traction-free surface as the system equilibrates. An insight to this observation may be seen from the following contour plots of normalized mean stress in the hydrogel.

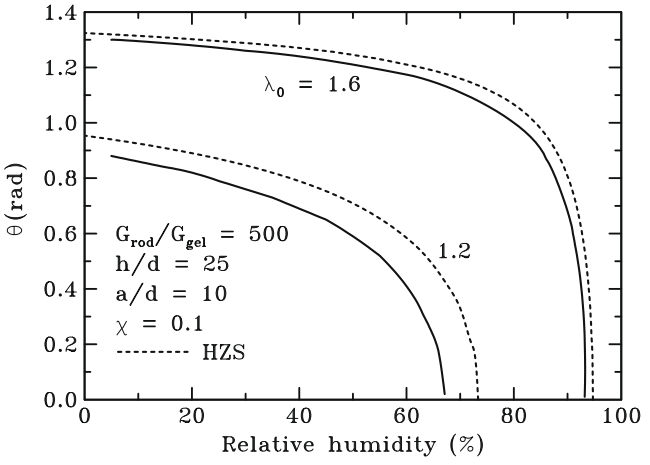

Fig. 4. Variation of tilt angle θ with humidity of environment RH for $\lambda_0 = 1.2$ and 1.6 with $G_{\text{rod}}/G_{\text{gel}} = 500$, $h/d = 25$, $a/d = 10$, $\chi = 0.1$. Solution from HZS is plotted alongside for comparison purposes and is shown as dotted line.

Fig. 5a and b shows the distributions of normalized mean stress σ_m/kT, where $\sigma_m = \sigma_{kk}/3$, in the tilted state along $X_1 - X_3$ plane for $X_2 = 0$ at RH of 50% for $\lambda_0 = 1.2$ and 1.6, with the equilibrium tilt angles at $\theta = 0.59$ rad and 1.2 rad, respectively. The contour plots shown in the figures are obtained by duplicating the contour plot of the RVE several times. Tensile stresses are developed near the surface of the hydrogel on the side of the inclined nanorods while compressive stresses are developed away from the surface and within the hydrogel. Maximum compressive stresses are generated at the bottom of the nanorods as they tilt. The mechanics of tilting can be understood as follows. The shrinking hydrogel exerts tensile forces. The nanorods, being modelled as stiff elements and undergo rigid body rotations, are loaded in compression and tend to redirect the tensile forces from the hydrogel, resulting in lateral tilt.

We observe from the surface profiles that troughs are formed on the top surface of the hydrogel, and that the deformations are asymmetric. These result from the traction-free condition imposed on the top surface. On this note, we wish to highlight that the solution from HZS can be obtained numerically if we prescribe displacements according to (7) to the boundaries of the model. This is, in effect, imposing a state of homogeneous deformation in the nanostructure. In doing so, the top surface will remain planar during deformation. Directing our attention to the surface profile of $\lambda_0 = 1.6$, it may be observed that the effect of the traction-free condition is somewhat negated due to the larger tilt angle θ. This effect probably results in the small deviation between solutions obtained numerically and from HZS. Inferring from this, we can predict that the solution for inhomogeneously deforming hydrogel will converge to that of homogeneously deforming hydrogel as λ_0 becomes larger ($\lambda_0 > 1.6$).

Corresponding to Fig. 5a and b, c and d displays, respectively, the tilted state of the nanostructure in the $X_1 - X_2$ plane (as viewed from top). The tilted nanorods form a patterned structure of uniform tilt direction. Such pattern has been demonstrated experimentally (see Fig. 4a of Sidorenko et al., 2007). In the figures shown, we duplicated, as done for Fig. 5a and b, the RVE to create an array of repetitive units to aid and enhance visualization of the geometry. Other patterns may be accomplished by varying, for instance, the exposed heights of the nanorods, periodicities and symmetries of the nanorods.

4.2. Tuning of adaptive response of nanostructure

It is clear, from the preceding section, that the adaptive response of the nanostructure can be tuned by controlling the degree of swelling of the hydrogel. In this section, we demonstrate the nanostructural parameters of nanorods' spacing a, shear modulus mismatch $G_{\text{rod}}/G_{\text{gel}}$ can be used to tune the adaptive behavior. For completeness, we include the material parameter of χ, the polymer–solvent interaction parameter for this parametric study. The results of the parametric study may provide a source of information for the designs of these nanostructures for specific applications.

Attention is first directed to the spatial distribution of the nanorods, specifically the spacing between adjacent nanorods. Fig. 6a shows the change in tilt angle θ in response to the humidity of the environment for varying normalized spacings a/d, for $\lambda_0 = 1.2$, $G_{\text{rod}}/G_{\text{gel}} = 500$, $h/d = 25$, $\chi = 0.1$. The dashed curve represents the bifurcation response from HZS. It is observed that both RH_c and tilt angle θ in the post-bifurcation regime decrease with increasing a/d. For a relative humidity of 10%, the tilt angles for $a/d = 10$, 20 and 30 are 0.86, 0.68 and 0.47 rad respectively. To elucidate the effects of

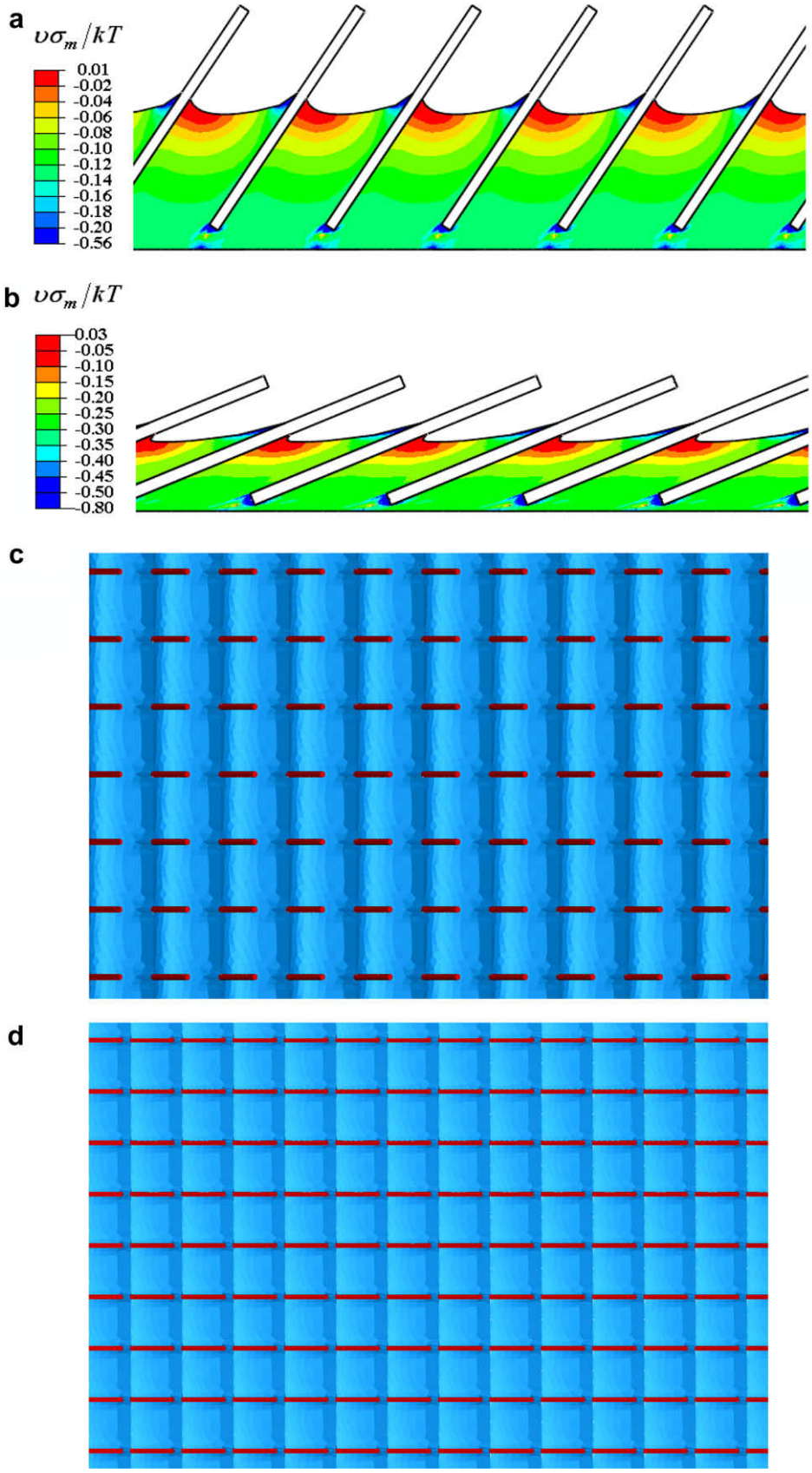

Fig. 5. Contour plots of normalized mean stress σ_m/kT along $X_1 - X_3$ plane for $X_2 = 0$ at relative humidity of 50% for (a) $\lambda_0 = 1.2$, equilibrium tilt angle $\theta = 0.59$ rad, and (b) $\lambda_0 = 1.6$, equilibrium tilt angle $\theta = 1.20$ rad (c) and (d) show the corresponding deformed patterns as viewed from the top for (a) and (b), respectively. Repetitive units of the representative volume element are made in the X_1- and X_2-directions with spacing a between adjacent units.

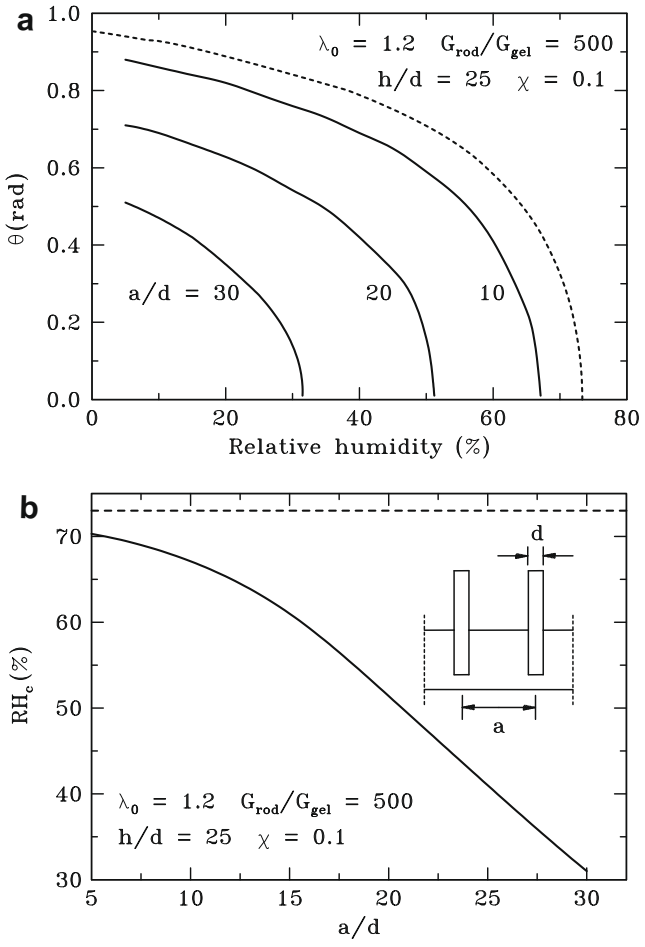

Fig. 6. (a) Effects of normalized spacings a/d on the variation of tilt angle θ with humidity of environment RH, and (b) plot of RH_c as a function of a/d, where analytical RH_c from HZS is represented by dotted line. $\lambda_0 = 1.2$, $G_{rod}/G_{gel} = 500$, $h/d = 25$, $\chi = 0.1$.

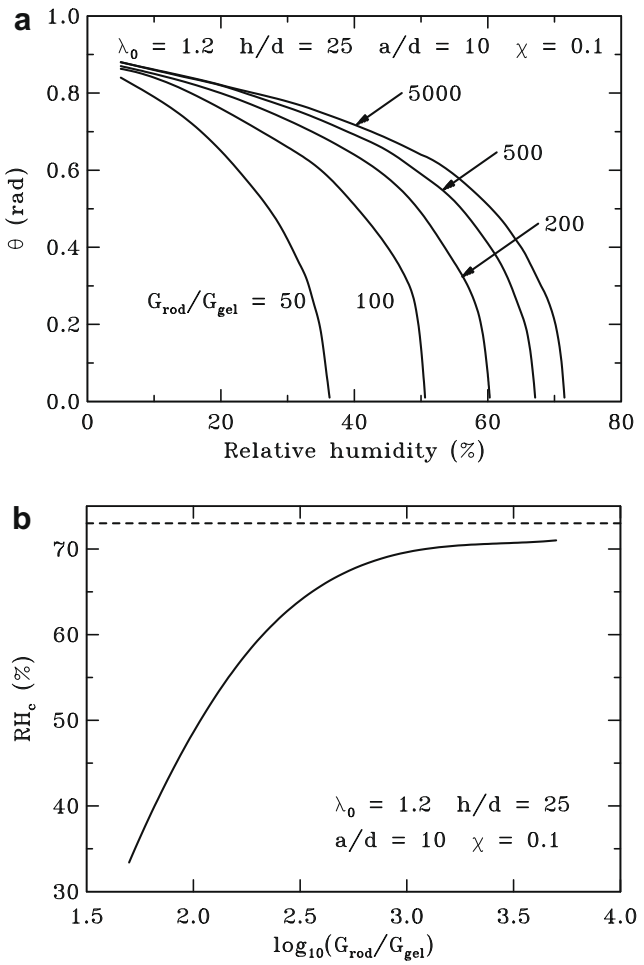

Fig. 7. (a) Effects of shear modulus mismatches G_{rod}/G_{gel} on the variation of tilt angle θ with humidity of environment RH, and (b) plot of RH_c as a function of G_{rod}/G_{gel}, where analytical RH_c from HZS is represented by dotted line. $\lambda_0 = 1.2$, $h/d = 25$, $a/d = 10$, $\chi = 0.1$.

a/d on RH_c, we plot the variation of RH_c with a/d, as demonstrated in Fig. 6b. The horizontal dotted line represents RH_c computed from HZS. RH_c is observed to relate linearly with a/d for $a/d > 15$. This relationship becomes nonlinear when the ratio falls below 15. It is seen that as a/d decreases, RH_c tends to the value predicted by HZS. We may infer from the two figures that as a/d decreases, the bifurcation response of the nanostructure with hydrogel undergoing inhomogeneous deformation converges to that with homogeneous hydrogel deformation. In the limiting case $a/d = 0$, the nanostructure effectively becomes a "sandwiched" structure, with a layer of hydrogel constraint to a silicon block on one side, and the stiff substrate on the other. However in reality, at low a/d the nanorods may actuate and tilt due to lateral adhesion between them (Pokroy et al., 2009) prior to any bifurcations due to humidity.

We next turn our attention to the dimensionless material parameter of G_{rod}/G_{gel}, the shear modulus mismatch between nanorod and the surrounding hydrogel. In this paper, the shear modulus of the nanorods is held constant while that of the hydrogel is varied. Values of $G_{rod}/G_{gel} = 50$ to $G_{rod}/G_{gel} = 5000$ are considered in this analysis. The aspect ratio of the nanorod h/d and the normalized spacing a/d are taken to be 25 and 10, respectively. The hydrogel has an initial swelling ratio $\lambda_0 = 1.2$.

Fig. 7a displays the response of tilt angle $\theta$with humidity of the environment RH for varying G_{rod}/G_{gel}. RH_c is seen to vary non-uniformly from approximately 36% for $G_{rod}/G_{gel} = 50$ to about 72% for $G_{rod}/G_{gel} = 5000$. Focusing on the post-bifurcation regime, it is observed that for the modulus mismatches considered, θ tends to a constant (close to 0.9 rad for the set of parameters considered in this case) as RH drops to zero, that is, a completely dry, water-free environment. A closer examination of the post-bifurcation regime in Fig. 7a reveals that the sensitivity of nanorods' tilting/switching to humidity decreases with increasing G_{rod}/G_{gel}. We define the tilt sensitivity as the change in θ for any given change in RH. This can be obtained graphically by constructing a tangent to each curve at any given RH. With a relative higher degree of stiffness of nanorod, larger forces need to be generated by the hydrogel for actuation. It is also noted that the range of humidity levels in which actuation can occur decreases with decreasing G_{rod}/G_{gel}. For example, a structure with $G_{rod}/G_{gel} = 50$ will have switching/actuation behavior in response to humidity levels between 0% and 36%, whereas for the case of $G_{rod}/G_{gel} = 5000$, between 0% and 72%. For any given humidity, for example 20%, a lower G_{rod}/G_{gel} results in a lower tilt angle.

Fig. 7b shows the relation between RH_c and G_{rod}/G_{gel}. RH_c from HZS is plotted as a horizontal dotted line. It is noted that for large G_{rod}/G_{gel}, the numerical solution of RH_c approaches that of the homogeneous solution predicted by HZS. From the plot, this convergence of solutions is expected to occur for $log_{10}G_{rod}/G_{gel} > 4$. This translates to a modulus mismatch of $G_{rod}/G_{gel} > 10^4$.

The results for the influence of χ on the bifurcation behavior are taken up next. χ, also known as the Flory interaction parameter, is

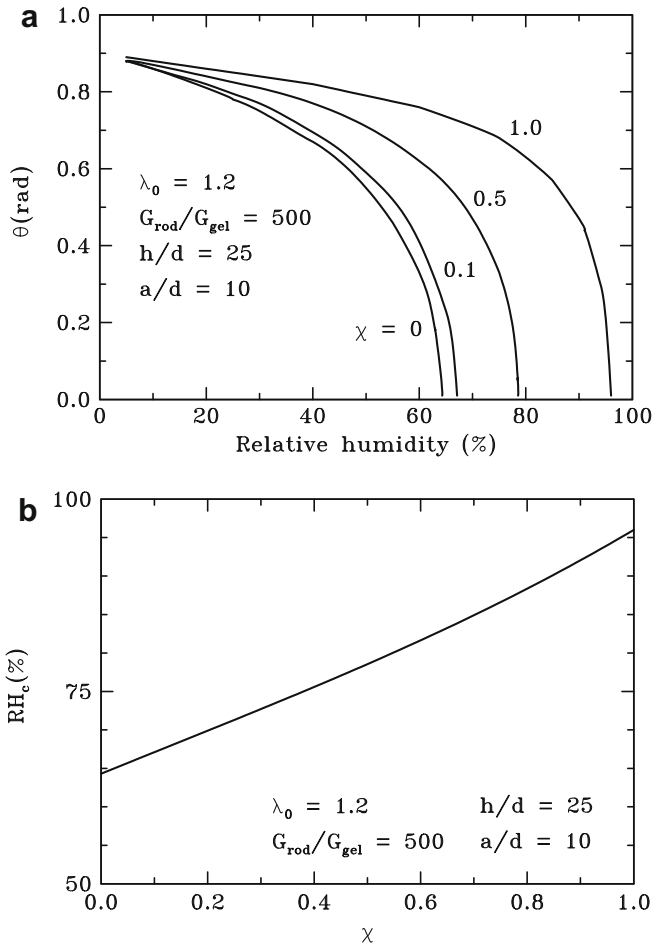

Fig. 8. (a) Effects of enthalpy of mixing χ on the variation of tilt angle θ with humidity of environment RH, and (b) plot of RH_c as a function of χ. $\lambda_0 = 1.2$, $G_{rod}/G_{gel} = 500$, $h/d = 25$, $a/d = 10$.

a dimensionless measure of enthalpy of mixing. It is a free-energy, material-specific parameter and it represents the polymer–solvent interaction, in this case the solvent being water. When $\chi > 0$, water molecules are motivated to leave the hydrogel. Fig. 8a shows the variation of tilt angle θ with humidity of the environment RH for several values of χ. Observe that the tilt angle θ approaches a constant, similar to the earlier study on the parameter of G_{rod}/G_{gel}. Without attaching physical/chemical significance of χ (we shall leave it to chemists and chemical engineers) RH_c is seen to increase as χ increases, with the corresponding increase in the range of humidity levels in which the actuation of nanorods can occur. Fig. 8b plots the variation of RH_c with χ and it shows the linear relationship between the two, with the curve attaining a plateau at $RH_c = 100\%$ for $\chi \gg 1.0$.

5. Concluding remarks

Integration of hard materials such as nanoscale silicon rods with stimuli-responsive polymer gels results in an adaptive structure that promises niche applications that are exciting and novel. In this paper, we have analysed the switching behavior of a hydrogel-based nanostructure subjected to drying conditions. A representative volume element is employed in this boundary value problem, wherein inhomogeneous deformation in the hydrogel and the nanostructural effects are accounted for. The inhomogeneity results in both a lowered critical humidity RH_c at which the nanorods stand vertical, and the tilt angle of the nanorods as a result of exposure to drying environment, in comparison to solutions predicted by HZS where homogeneous deformation of hydrogel is assumed. In particular, the HZS solutions provide upper bounds to the bifurcation behaviors of the nanostructure in study. Numerical results show that at higher initial stretch ratio, the bifurcation behavior of the nanostructure approaches that of the HZS solution.

We also analyse the effects of several geometric-material parameters on the bifurcation behavior; the spacing between adjacent nanorods a/d, shear moduli mismatch G_{rod}/G_{gel} and the enthalpy of mixing χ. Each of these parameters shows significant influence on the critical humidity and post-bifurcation behavior. Increasing a/d, or decreasing G_{rod}/G_{gel} or χ all have an effect of lowering the critical humidity. These parameters can be exploited to tune the adaptive response of the nanostructure for specific applications. The list of geometric-material parameters affecting the critical humidity and post-bifurcation behavior highlighted in this paper is by no means exhaustive. Other parameters may include the aspect ratio and non-circular cross-section of the nanorods. These factors are the focus of future research to provide a more complete list of parameters so as to aid in the design and application of these adaptive nanostructures.

In the hybrid architecture considered in this paper, the nanorods are free-standing. Another design architecture developed and investigated by Sidorenko et al. (2007) has the nanorods attached to the substrate. The mechanisms of tilt and deformation of the nanorods are different. In the design, the nanorods do not carry compressive loads and undergo rigid body rotation upon actuation as in the case of free-standing nanorods; they bend instead. The numerical analysis of this boundary value problem will be different; the use of representative volume element and periodic boundary conditions may no longer be applicable. Instead, a full-field analysis of the whole structure may be required and this presents a scientific and computational challenge. This is a rich area of future research.

Acknowledgment

The support of this work by the National University of Singapore is gratefully acknowledged.

References

Ahn, S.K., Kasi, R.M., Kim, S.C., Sharma, N., Zhou, Y.X., 2008. Stimuli-responsive polymer gels. Soft Matter 4, 1151–1157.
Autumn, K., Sitti, M., Liang, Y.A., Peattie, A.M., Hansen, W.R., Spoonberg, S., Kenny, T.W., Fearing, R., Israelachvili, J.N., Full, R.J., 2002. Evidence for van der Waals adhesion in gecko setae. PNAS 99, 12252–12256.
Barthlott, W., Neinhuis, C., 1997. Purity of the sacred lotus, or escape from contamination in biological surfaces. Planta 202, 1–17.
Beebe, D.J., Moore, J.S., Bauer, J.M., Yu, Q., Liu, R.H., Devadoss, C., Jo, B.H., 2000. Functional hydrogel structures for autonomous flow control inside microfluidic channels. Nature 404, 588–590.
Birgersson, E., Li, H., Wu, S., 2008. Transient analysis of temperature-sensitive neutral hydrogels. J. Mech. Phys. Solids 56, 444–466.
De, S.K., Aluru, N.R., Johnson, B., Crone, W.C., Beebe, D.J., Moore, J., 2002. Equilibrium swelling and kinetics of pH-responsive hydrogels: models, experiments, and simulations. J. Microelectromech. Syst. 11, 544–555.
Dolbow, J., Fried, E., Ji, H., 2004. Chemically induced swelling of hydrogels. J. Mech. Phys. Solids 52, 51–84.
Flory, P.J., Rehner, J., 1943. Statistical mechanics of cross-linked polymer networks II: Swelling. J. Chem. Phys. 11, 521–526.
Geim, A.K., Dubonos, S.V., Grigorieva, I.V., Novoselov, K.S., Zhukov, A.A., Shapocal, S.Y., 2003. Microfabricated adhesive mimicking gecko foot-hair. Nat. Mater. 2, 461–463.
Hirai, T., 2007. Electrically active non-ionic artificial muscle. J. Intel. Mat. Syst. Str. 18, 117–122.
Hong, W., Zhao, X., Suo, Z., 2008a. Drying-induced bifurcation in a hydrogel-actuated nanostructure. J. Appl. Phys. 104, 084905.
Hong, W., Zhao, X., Zhou, J., Suo, Z., 2008b. A theory of coupled diffusion and large deformation in polymeric gels. J. Mech. Phys. Solids 56, 1779–1793.
Hong, W., Liu, Z., Suo, Z., 2009. Inhomogeneous swelling of a gel in equilibrium with a solvent and mechanical load. Int. J. Solids Struct. 46, 3282–3289.

Ji, H., Mourad, H., Fried, E., Dolbow, J., 2006. Kinetics of thermally induced swelling of hydrogels. Int. J. Solids Struct. 43, 1878–1907.
Li, H., Luo, R., Birgersson, E., Lam, K.Y., 2007. Modeling of multiphase smart hydrogels responding to pH and electric voltage coupled stimuli. J. Appl. Phys. 101, 114905.
Li, H., 2009. Smart Hydrogel Modelling. Springer, Berlin.
Osada, Y., Okuzaki, H., Hori, H., 1992. A polymer gel with electrically driven motility. Nature 355, 242–244.
Osada, Y., Matsuda, A., 1995. Shape memory in hydrogels. Nature 376, 219.
Pardo-Yissar, V., Gabai, R., Shipway, A.N., Bourenko, T., Willner, I., 2001. Gold nanoparticles/hydrogel composites with solvent-switchable electronic properties. Adv. Mater. 13, 1320–1323.
Pokroy, B., Epstein, A.K., Persson-Gulda, M.C.M., Aizenberg, J., 2009. Fabrication of bioinspired actuated nanostructures with arbitrary geometry and stiffness. Adv. Mater. 21, 463–469.
Russell, T.P., 2002. Surface-responsive materials. Science 297, 964–967.
Sidorenko, A., Krupenkin, T., Taylor, A., Fratzl, P., Aizenberg, J., 2007. Reversible switching of hydrogel-actuated nanostructures into complex micropatterns. Science 315, 487–490.
Sidorenko, A., Krupenkin, T., Aizenberg, J., 2008. Controlled switching of the wetting behavior of biomimetic surfaces with hydrogel-supported nanostructures. J. Mater. Chem. 18, 3841–3846.
Zhang, J., Zhao, X., Suo, Z., Jiang, H., 2009. A finite element method for transient analysis of concurrent large deformation and mass transport in gels. J. Appl. Phys. 105, 093522.
Zhao, X., Hong, W., Suo, Z., 2008. Inhomogeneous and anisotropic equilibrium state of a swollen hydrogel containing a hard core. Appl. Phys. Lett. 92, 051904.